AD_____

Award Number: DAMD17-99-1-9555

TITLE: Evaluation of Early and Prolonged Effects of Acute
Neurotoxicity and Neuroprotection Using Novel Functional Imaging
Techniques

PRINCIPAL INVESTIGATOR: Dr. Anna-Liisa Brownell

CONTRACTING ORGANIZATION: The General Hospital Corporation
Boston, Massachusetts 02114

REPORT DATE: August 2001

TYPE OF REPORT: Annual

PREPARED FOR: U.S. Army Medical Research and Materiel Command
Fort Detrick, Maryland 21702-5012

DISTRIBUTION STATEMENT: Approved for Public Release;
Distribution Unlimited

The views, opinions and/or findings contained in this report are
those of the author(s) and should not be construed as an official
Department of the Army position, policy or decision unless so
designated by other documentation.

REPORT DOCUMENTATION PAGE

1. AGENCY USE ONLY (Leave blank)	2. REPORT DATE August 2001	3. REPORT TYPE AND DATES COVERED Annual (15 Jul 00 – 15 Jul 01)

4. TITLE AND SUBTITLE
Evaluation of Early and Prolonged Effects of Acute Neurotoxicity and Neuroprotection Using Novel Functional Imaging Techniques

5. FUNDING NUMBERS
DAMD17-99-1-9555

6. AUTHOR(S)
Dr. Anna-Liisa Brownell

7. PERFORMING ORGANIZATION NAME(S) AND ADDRESS(ES)

The General Hospital Corporation
Boston, Massachusetts 02114

E-Mail: abrownell@partners.org

8. PERFORMING ORGANIZATION REPORT NUMBER

9. SPONSORING / MONITORING AGENCY NAME(S) AND ADDRESS(ES)

U.S. Army Medical Research and Materiel Command
Fort Detrick, Maryland 21702-5012

10. SPONSORING / MONITORING AGENCY REPORT NUMBER

20011127 045

11. SUPPLEMENTARY NOTES
Report contains color

12a. DISTRIBUTION / AVAILABILITY STATEMENT
Approved for Public Release; Distribution Unlimited

12b. DISTRIBUTION CODE

13. Abstract *(Maximum 200 Words) (abstract should contain no proprietary or confidential information)*

Increasing environmental toxicity has been significantly linked either directly, or indirectly, to the etiology of neurodegenerative diseases. We have proposed to explore the relationship between impairments in functional and metabolic pathways and regional neural dysfunction, and the efficacy of neuroprotection provided by a metabotropic glutamate receptor agonist. We have conducted studies of dopamine receptors, reuptake sites, metabotropic glutamate receptors and glucose metabolism using a super-high resolution positron tomograph to explore acute and long-term excitotoxicity mediated mechanisms in rats exposed to 3-nitroproprionic acid (3-NP). We have also conducted studies of glucose metabolism in transgenic mice expressing Huntington's gene. Complementary magnetic resonance spectroscopy studies to explore changes in neurochemicals were conducted in both 3-NP treated rats and transgenic mice as well. A significant amount of biological information has been obtained regarding 3-NP induced degenerative changes in energy metabolism and dopaminergic regulation. Interanimal variability of motor activity and glucose metabolism in response to 3-NP continue. Studies of dopamine receptors (D1 and D2) showed a gradual decrease following 3-NP administration. An early increase in dopamine transporter binding to presynaptic terminals was observed immediately after 3-NP, followed by a gradual decrease. Studies of glutamate receptors showed locally decreased binding in striatum and in cortex following 3-NP. Reversible early increases of lactate and succinate in MRS were observed as well. In addition, technical goals of algorithm development for data acquisition, image reconstruction, and data analyses were met.

14. Subject Terms (keywords previously assigned to proposal abstract or terms which apply to this award)
neurotoxin, positron emission tomography, glucose metabolism, dopamine receptors, glutamate receptors, metabotropic glutamate

15. NUMBER OF PAGES
34

16. PRICE CODE

17. SECURITY CLASSIFICATION OF REPORT	18. SECURITY CLASSIFICATION OF THIS PAGE	19. SECURITY CLASSIFICATION OF ABSTRACT	20. LIMITATION OF ABSTRACT
Unclassified	Unclassified	Unclassified	Unlimited

Table of Contents

SECOND ANNUAL REPORT "Evaluation of Early and Prolonged Effects of Acute Neurotoxicity and Neuroprotection Using Novel Functional Imaging Techniques"

INTRODUCTION

Exogenous and/or endogenous neurotoxicity has directly or indirectly related to various neurodegenerative diseases including Parkinson's and Huntington's disease (Reiter et al 1998, Gorrell et al 1996, Zayed et al 1996). Therefore it is a major challenge to develop specific and sensitive in vivo methods to investigate pathophysiological mechanisms of toxins. This information is essential in order to design new methods for neuroprotection and therapy. Our overall research goal in the project is to develop and improve in vivo imaging techniques to examine the neuro-function of glutamatergic and dopaminergic receptors as well as oxidative glucose metabolism and neurochemicals. We particularly focus our efforts in exploring the excitotoxicity induced regional neuronal dysfunction in functional and metabolic pathway. The neuronal toxicity models include 3-nitropropionic acid induced striatal lesions and transgenic mice with gene expression of human Huntington's disease (HD). In the final phase of this project we will test neuroprotection with novel newly developed metabotropic glutamate receptor agonist.

BODY

The second grant year included longitudinal imaging studies in HD models with 3-nitropropionic (3-NP) rats and HD transgenic mice. In addition, further development of super-high resolution PET imaging techniques was conducted to enable to produce highly repeatable imaging studies in longitudinal imaging sessions. Also significant development of radiolabeling of metabotropic glutamate receptors was done. Progress in the different areas is evaluated in the following.

1. Technical tasks: Further development of imaging techniques was conducted during the second grant year. These tasks included further development of a computer driven imaging table for the super-high resolution positron emission tomography (PET) device and further development of software for data acquisition, implementation of image reconstruction programs to the unix (linux) based computer system and development of image analyses for multimodality data co-registration.

a) **Computer controlled imaging "table":** During the first grant year we developed a basic model of computer controlled imaging "table" for the small super-high resolution positron emission tomograph. During the second grant year we further optimized it. The "table", which includes a stereotactic headholder with earbars and mouth (teeth) bar is designed separately for rat and mouse (Figure 1, Appendix) because the size of the head of these two species is significantly different as well as the other experimental maneuvering to prepare animals for imaging studies. In addition, during the longitudinal follow up studies of up to 4 months the body size of

4

rat will be doubled and therefore we had to do an improved design for the imaging table of rat, which allows the body size to increase without limits.

b) **Software development:** Software was developed to control the movement of the imaging "table" electronically to scan through the whole brain slice by slice. Image reconstruction programs have also been updated and further developed to run in modern high speed PC computers, both in windows and unix (linux) based system.

The computer system controlling the PET device is a window PC system and PET data is obtained in an in-house developed PC data format. Magnetic resonance imaging and spectroscopy (MRS) are acquired using unix based systems. To be able to perform image comparison and data fusion of PET and MRI/MRS we have developed further programs to make PET data compatible to the systems.

The other challenge in software development has been to develop high resolution imaging techniques for multimodality registration. The technique we are using now is based on volume rendering of MR images and fusion of MR and PET images based on the Normalized Mutual Information (NMI) algorithm (Figures 2, Appendix)

2) **Radiopharmaceutical development:** Dr. Alan Kozikowski has synthetized and provided us the precursor for labeling of metabotropic glutamate receptor agonist; ABHx-D-I. This ligand binds both on group I and II metabotropic glutamate receptors. Reported EC50 values are mGluR2 (0.33uM) > mGluR5 (0.72 uM) > mGluR1 (1.6 uM) > mGluR3 (2.2 uM) > mGluR6 (5.3) > mGluR4 (23 uM) (Kozikowski et al1998, Conti et al 2000). We have developed radiolabeling with carbon-11 to obtain high specific activity. High specific activity is needed to introduce necessary radioactivity level into the target to produce statistically meaningful images. In small animal models one of restricting factors is that only limited volume of labeled ligand can be administered intravenously.

3) **Biological experiments:**

a) **Experimental animals:** During the second year, longitudinal imaging studies were conducted in 28 rats (male Spraque-Dawley) and 30 HD transgenic and 8 littermate mice. Altogether 119 PET imaging sessions and 46 MRI-MRS imaging sessions were conducted.

b) **Procedures in rats:** Twenty five rats were administered with 3-NP (10 mg/kg i.p., 2 times a day for 5 days or until symptomatic (gait observed). During the 3-NP treatment period, rats were individually housed in the metabolic cages, and their diet and excretion was closely followed. For imaging studies rats were anesthetized with halothane (1-1.5% with oxygen flow rate of 3 L/min). Catheters were introduced into the tail vein for administration of labeled ligands and into the tail artery for blood

5

samples to determine glucose level and blood input function needed for quantification of glucose metabolic rate and/or receptor binding.

c) **Results in rats:** *Weight and behavior*: There was a significant interanimal variability in response to 3-NP toxication on locomotor activity. In addition, the animals with strongest response to 3-NP lost about 30 % of their weight and the weight loss extended 4-5 days after neuroxicity. The observations in motor activity are similar to the results published by Borlongan et al 1997, Guyot et al 1997 and Eradiri et al 1999.

Imaging studies of glucose metabolism: PET imaging studies of glucose metabolism were conducted using ^{18}F-2-fluorodeoxy-D-glucose as tracer in eight 3-NP treated rats before and during 3-NP administrations, and 2 days, 4 weeks and 4 months post 3-NP.

In the daily PET imaging studies during 3-NP administration, we found significant interanimal variation in glucose metabolism, which is correlated to the motor activity. The animals which showed hindlimb paralyses had extensive striatal lesions. The average decrease of glucose utilization in these lesions was 40-50 % compared to normal striata and these lesions were developed a day after starting 3-NP.

Follow-up studies of glucose utilization after cessation of 3-NP showed an initial recovery from the acute phase and then decline again (2 days; -31+/-12 %, 4 weeks; -13+/-5 %, and 4 months; - 48+/-10% (Figure 3, Appendix).

Since glucose utilization is a major energy source of the brain, the change in glucose utilization can be a sensitive indicator for the energy dysfunction in the brain. 3-NP, a permanent inhibitor of succinate dehydrogenese (Johnson et al 2000) can disrupt the mitochondrial function, decrease glucose utilization and cause striatal degeneration (Storgaard et al 2000, Guyot et al 1997, Bowyer et al 1996). Therefore, to estimate the functional damage in brain we performed an additional study of glucose utilization in all rats 2 days after 3-NP administrations.

Imaging studies of dopamine receptors: We conducted imaging studies of dopamine D1 and D2 receptors and dopamine transporters in 12 rats before 3-NP injections and 2days, 4 weeks and 4 months post 3-NP. Dopamine D1 receptors were imaged with ^{11}C-SCH (Schoering 23660) and dopamine D2 receptors with ^{11}C-raclopride. Dopamine transporters were imaged with ^{11}C-CFT (2β-carbomethoxy-3β-(4-fluorophenyl tropane). Because of the interanimal variation of the response of 3-NP toxicity, a study of glucose utilization was conducted 2 days after 3-NP to estimate brain damage. Small decrease in dopamine D1 and D2 receptor bindings (4+/-2 % and 5+/-2 %, respectively) were observed 2 days after 3-NP. In 4 weeks, more severe decreases in dopamine D1 and D2 receptor bindings were observed (-24+/-8 % and -23+/-7 %, correspondingly). After that gradual depletion of dopaminergic system continued and dopamine D1 and D2 receptor binding 4 months after 3-NP (36+/-9 and 33+/- 8 % correspondingly). Interestingly, dopamine transporter binding imaged by ^{11}C-CFT showed early increase 2 days after 3-NP administrations (6+/-3%). After that moderate decrease was observable: -10+/-3% in 4 weeks and -12+/-4% in 4

6

months (Figure 3, Appendix). There are also some interesting publications of dopamine toxicity and correlation to 3-NP toxicity. Reynolds et al (Reynolds et al 1998) published that dopamine deficiency may protect against 3-NP toxicity and Johnson et al (Johnson et al 2000) published that long term exposure to 3-NP increases dopamine turnover.

Imaging studies of metabotropic glutamate receptors: After a long and tedious process a method was developed for labeling of an agonist for metabotropic glutamate receptors. The distribution of the labeled ligand was investigated in 3 control rats (Figure 4, Appendix) and imaging studies of metabotropic glutamate receptors (mGluR) were conducted in 5 rats pre and post 3-NP (3 days and 4 weeks post 3-NP). For comparison metabotropic glutamate receptor distribution was compared to the study of glucose utilization (Figure 5, Appendix). Glucose study confirms deficiency of MGluR binding in striata after 3-NP. In addition, metabotropic glutamate receptor binding is also decreased in cortical areas. For comparison one imaging study of glutamate receptors was conducted in one quinolinic acid lesioned rat to demonstrate a local defect in metabotropic glutamate receptor binding (Figure 6, Appendix).

Imaging studies of anatomy and neurochemicals (MRI/MRS studies): Imaging studies of neuroanatomy has been used to identify location and size of lesions and for volumetric image rendering. MRS studies of neurochemicals showed elevated peaks of lactate and macromolecules as well as succinate immediately after 3-NP toxicity (Figure 7, Appendix). These peaks diminished in 4 months, indicating a reversible process. Choline (Cho) peak increased and N-acetylaspartate peak decreased in 4 months indicating loss and damage of neurons. Similar observations of this temporal change in neurochemicals after acute 3-NP intoxication has been published by Lee (Lee et al 2000) (Figure 8, Appendix).

Histological confirmation of neural loss: Histological endpoint studies were conducted in 12 rats to confirm the neural loss. Figure 9 (Appendix) shows an endpoint study of glucose utilization and its corresponding Nissl stained tissue cut.

d) **Imaging studies in mice:** We conducted longitudinal imaging studies of glucose metabolism in control and Huntington's disease mouse model to optimize technical aspects and evaluate age related correlation of glucose metabolism. Figure 10 (Appendix) shows studies of glucose metabolism imaged using [18]F-2FDG and super-high resolution PET system in a control littermate and HD mouse at two different age points. The slice thickness is 1.5 mm and studies were performed with 1.25 mm steps. For MRS, the imaging voxels were placed symmetrically over both basal ganglia (average size of 6x3.5x3mm, 63uL) or over the motor cortex (6x2x3 mm, 36uL). Spectra were integrated and normalized to the creatine/phosphocreatine peak. Longitudinal analyses of glucose utilization in HD mice showed in striatum a progressive decrease of 0.05%/day. The decrease in the striatal NAA (0.56%/day) was one order higher than the glucose utilization (Figure 10, Appendix). In the same time period, Cho was increased 34 % compared to the littermate control. These

7

observations parallel the developing of HD symptoms. Interestingly, no significant changes were observed in cortical metabolism (Figure 11, Appendix).

KEY RESEARCH ACCOMPLISHMENT

-   further enhancement of imaging "tables" with stereotactic headholders for rat and mouse

-   further development of software for data acquisition and reconstruction for modern PC and linux based systems

-   further development and testing image algorithms for image reconstruction for multi modality image co-registration

-   observation of significant interanimal variation in the response to 3-NP induced neurotoxicity in motor activity and energy metabolism

-   observation that striatal lesion in glucose (energy) metabolism can be introduced immediately after first administration of 3-NP

-   observation that striatal lesions with energy deficit show progressive decrease in dopamine D1 and D_2 receptor

-   observation that dopamine transporter binding is slightly increased immediately after 3-NP treatment and progressively decreases later

-   observation that after 3-NP treatmentmetabotropic glutamate receptor binding is decreased focally in striatal area which also showed decreased glucose utilization

-   observation that MRS shows increased succinate and lactate and macromolecules in early 3-NP toxication and these are reversible changes

-   observation that decreasing of glucose utilization as well as NAA is linearly correlated with age in the striatum of HD mice

REPORTABLE OUTCOME

A-L. Brownell, Y.I. Chen, K.E. Canales, R.T. Powers, A.Dedeoglu, B.G. Jenkins. Coupling of glucose utilization to neuronal toxicity – an ultra high resolution PET study. The 48th Annual Meeting of the Society Nuclear Medicine. Toronto, Canada, June 23-27, 2001. Journal of Nuclear Medicine 42:215P, 2001

A-L Brownell, YI Chen, KE Canales, RT Powers, A Dedeoglu, FM Beal, BG Jenkins. 3-NP induced neurotoxicity – assessed by ultra high resolution PET with comparison to

MRI and MRS. 31st Annual Meeting of Neuroscience. San Diego, November 10-15, 2001.

Anna-Liisa Brownell, Y. Iris Chen, Kelly Canales, Robert Powers, Ole Andreasson, Flint Beal, Bruce Jenkins. Glucose utilization assessed by high resolution PET with comparison to MRI/MRS in a transgenic mouse model of Huntington's disease. HiRes2001, Meeting on High Resolution Imaging in Small Animals: Instrumentation, Applications and Animal Handling, September 9-11,2001, Rockville, Maryland.

T. Cao-Huu, A-L. Brownell. Multiresolution estimation. IEEE Imaging Conference. San Diego, November 2001.

Manuscripts under process:

Meixiang Yu, Y. Iris Chen, Kelly E. Canales, Elijahu Livni, Kjell Nagren, Alan P. Kozikowski, David R. Elmaleh, Anna-Liisa Brownell. C-11 labelling and in vivo evaluation of [11C] (1S2S4S5S) dimethyl 2-(methylamino) bicyclo[2.1.1]hexane-2,6-dicarboxylate. To be submitted to the Journal of Neurochemistry.

A-L Brownell, YI Chen, KE Canales, RT Powers, A Dedeoglu, FM Beal, BG Jenkins. 3-NP induced neurotoxicity – assessed by ultra high resolution PET with comparison to MRI and MRS. To be submitted to the Journal of Neuroscience.

CONCLUSIONS

The second grant year has been very successful and significant amount of biological information has been obtained regarding the 3-NP induced degenerative processes in energy metabolism as well as dopaminergic regulation during degeneration. We observed increase in dopamine transporter binding to presynaptic terminals immediately after 3-NP intoxication. This phenomen as well as early increases of lactate and succinate in MRS were reversible. Metabotropic glutamate receptors provide a new interesting insight to investigate the degenerative processes and their neuroprotective characteristics will be investigated in the coming years. During the second year, a number of technical tasks have also been accomplished including further development of computer controlled imaging "table" and other accessories needed to accomplish the whole project. Algorithm development for data acquisition, image reconstruction and data analyses have been very successful and automated programs are now running both in windows and linux based systems.

REFERENCES

Borlongan CV, Koutouzis TK, Freeman TB, Hauser RA, Cahill DW, Sanberg PR. Hyperactivity and hypoactivity in a rat model of Huntington's disease: the systemic 3-nitropropionic acid model. Brain Res Brain Res Protoc 1997;1(3):253-7.

Bowyer JF, Clausing P, Schmued L, Davies DL, Binienda Z, Newport GD, Scallet AC, Slikker W Jr. Parenterally administered 3-nitropropionic acid and amphetamine can combine to produce damage to terminals and cell bodies in the striatum. Brain Res 1996; 712(2):221-9.

Conti P, Kozikowski AP. New synthesis of 2-aminobicyclo[2.1.1]hexane-2,5-dicarboxylic acid-I (ABHxD-I), a potent metabotropic receptor agonist. Tetrahedron Letters 0 (2000) 1-4.

Eradiri OL, Starr MS. Striatal dopamine depletion and behavioural sensitization induced by methamphetamine and 3-nitropropionic acid. Eur J Pharmacol 1999; 386(2-3):217-26.

Gorrell JM, DiMonte D, Graham D. The role of the environment in Parkinson's disease. Environmental Health Perspective1996; 104: 652-4.

Guyot MC, Hantraye P, Dolan R, Palfi S, Maziere M, Brouillet E. Quantifiable bradykinesia, gait abnormalities and Huntington's disease-like striatal lesions in rats chronically treated with 3-nitropropionic acid. Neuroscience 1997; 79(1):45-56.

Johnson JR, Robinson BL, Ali SF, Binienda Z. Dopamine toxicity following long term exposure to low doses of 3-nitropropionic acid (3-NPA) in rats. Toxicol Lett 2000; 116(1-2):113-8.

Kozikowski AP, Steensma D, Araldi GL, Tuckmantel W, Wang S, Pshenichkin S, Surina E, Wroblewski JT. Synthesis and biology of the conformationally restricted ACPD analogue, 2-aminobicyclo[2.1.1]hexane-2,5-dicarboxylic acid-I, a potent mGluR agonist. J Med Chem 1998; 41,1641-1650.

Lee W-T, Lee C-S, Pan Y-L, Chang C. Temporal changes of cerebral metabolites and striatal lesions in acute 3-nitropropionic acid intoxication in the rat. Magnetic Resonance in Medicine 2000; 44: 29-34.

Reiter LM, DeRosa C, Kavlock RJ, Lucier G, Mac MJ, Melillo J, Melnick RL, Sinks T, Walton BT, The U.S. Federal framework for research on endocrine disruptors and an analysis of research programs supported during fiscal year 1996. Environmental Health Prespect 1998; 106: 105-113.

Reynolds DS, Carter RJ, Mortion AJ. Dopamine modulates the susceptibility of striatal neurons to 3-nitropropionic acid in the rat model of Huntington's disease. J Neurosci 1998; 18(23)1011-27.

Storgaard J, Kornblit BT, Zimmer J, Bert J, Gramsbergen P. 3-Nitropropionic acid in organotypic striatal and corticostriatal slice cultures is dependent on glucose and glutamate. Exp Neurol 2000; 164(1):227-35.

Zayed J, Mikhail M, Loranger S, Kennedy G, L'Esperance G. Exposure of taxi drivers and office workers to total and respirable manganese in an urban environment. American Industrial Hygiene Association Journal 1996; 57: 376-80.

APPENDICES

Figures 1-11.

Abstracts and reports:

A-L. Brownell, Y.I. Chen, K.E. Canales, R.T. Powers, A.Dedeoglu, B.G. Jenkins. Coupling of glucose utilization to neuronal toxicity – an ultra high resolution PET study. The 48th Annual Meeting of the Society Nuclear Medicine. Toronto, Canada, June 23-27, 2001. Journal of Nuclear Medicine 42:215P, 2001

A-L Brownell, YI Chen, KE Canales, RT Powers, A Dedeoglu, FM Beal, BG Jenkins. 3-NP induced neurotoxicity – assessed by ultra high resolution PET with comparison to MRI and MRS. 31st Annual Meeting of Neuroscience. San Diego, November 10-15, 2001

Anna-Liisa Brownell, Y. Iris Chen, Kelly Canales, Robert Powers, Ole Andreasson, Flint Beal, Bruce Jenkins. Glucose utilization assessed by high resolution PET with comparison to MRI/MRS in a transgenic mouse model of Huntington's disease. HiRes2001, Meeting on High Resolution Imaging in Small Animals: Instrumentation, Applications and Animal Handling, September 9-11,2001, Rockville, Maryland.
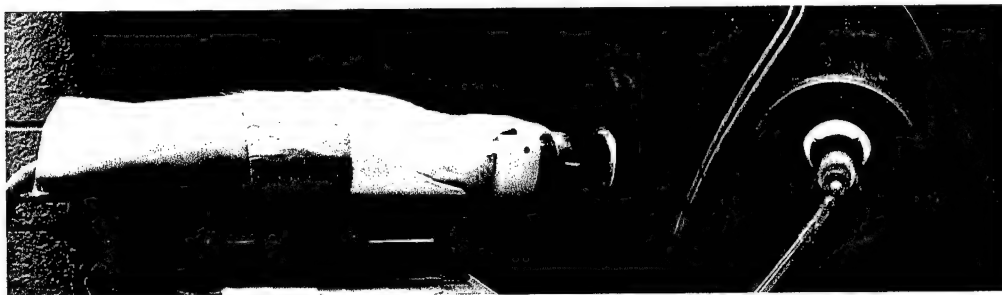
T. Cao-Huu, A-L. Brownell. Multiresolution estimation. IEEE Imaging Conference. San Diego, November 2001.

PI. Anna-Liisa Brownell: "Evaluation of Early and Prolonged Effects of Acute Neurotoxicity Using Novel Functional Imaging Techniques"

Rat and mouse frames used for PET studies
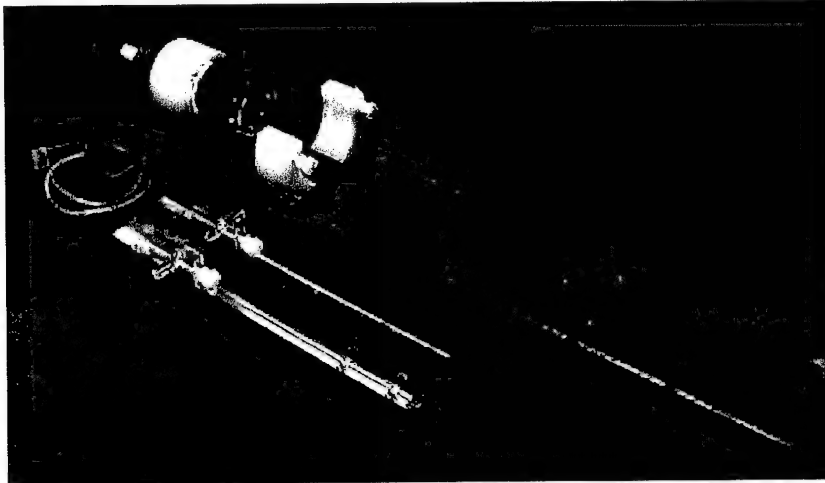
Rat experiment in a super high resolution PET camera

Side View   **Front View**

Figure 1. Stereotactic headholders for mouse and rat and experimental arrangement for PET imaging.
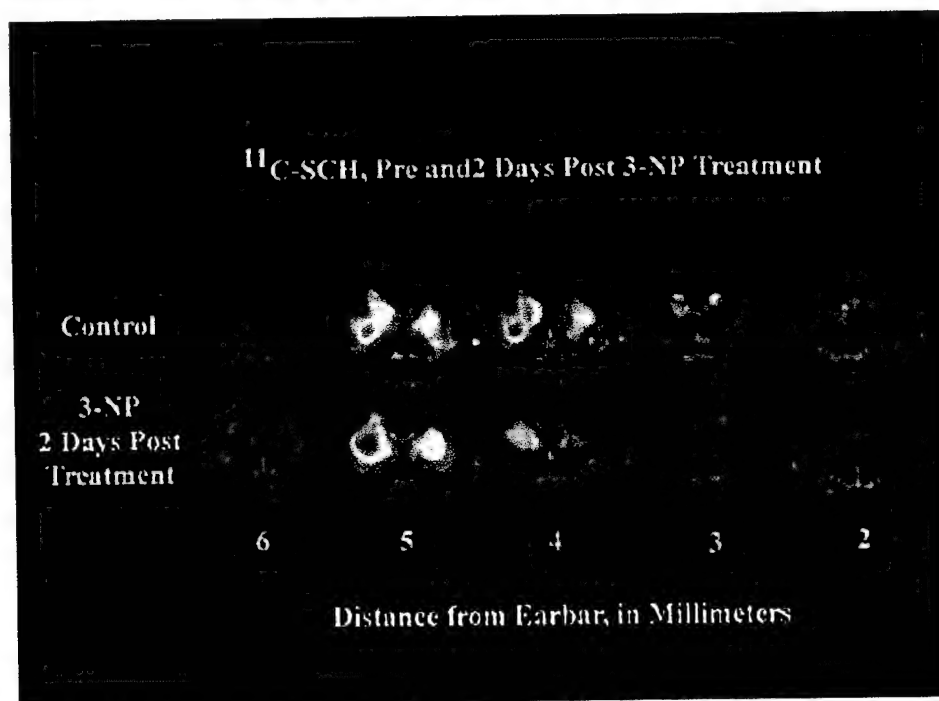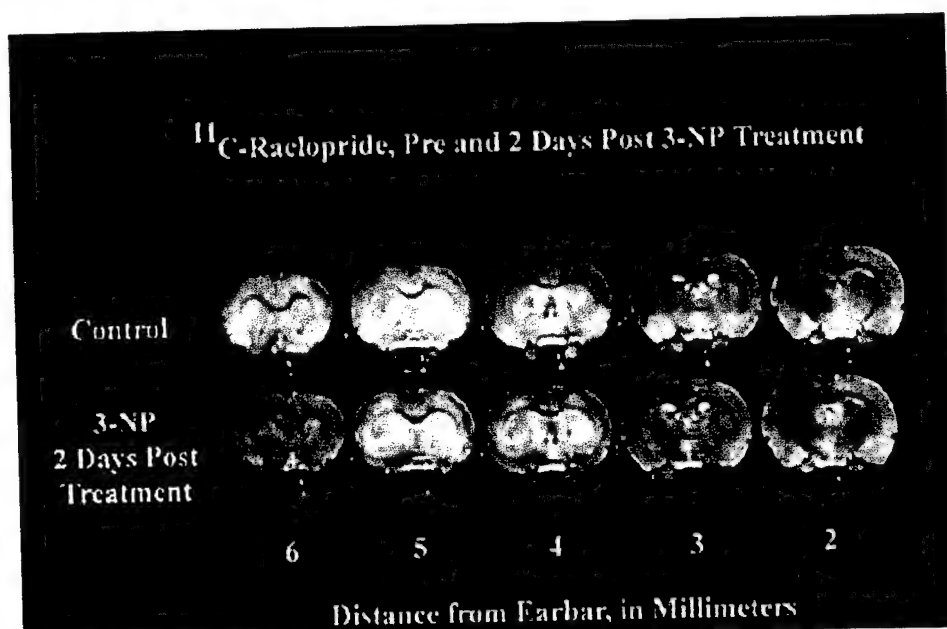
Figure 2. Volume rendered MR images fused with PET images showing dopamine D2 receptor binding (^{11}C-raclopride), dopamine D1 receptor binding (^{11}C-SCH) and dopamine transporter binding in presynaptic terminals (^{11}C-CFT) in the same animal pre and 2days post 3-NP.
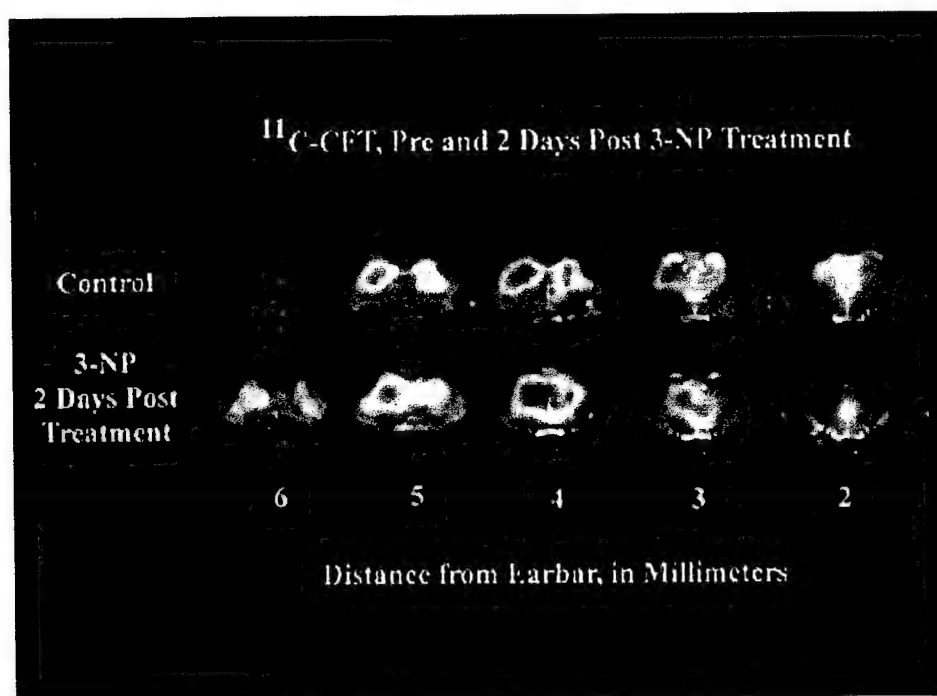
Figure 2 cont. Volume rendered MR images fused with PET images showing dopamine D2 receptor binding (^{11}C-raclopride), dopamine D1 receptor binding (^{11}C-SCH) and dopamine transporter binding in presynaptic terminals (^{11}C-CFT) in the same animal pre and 2days post 3-NP.
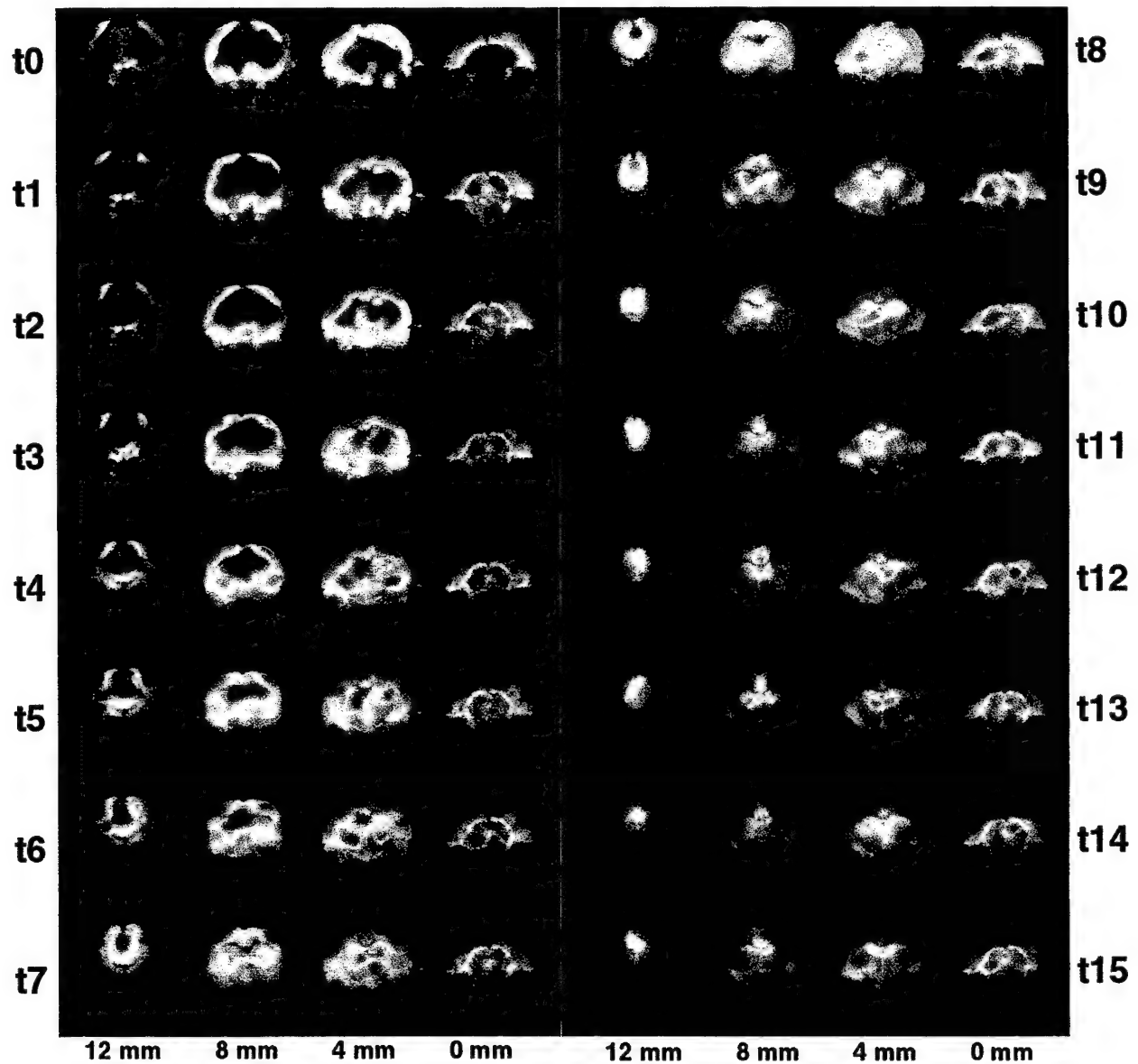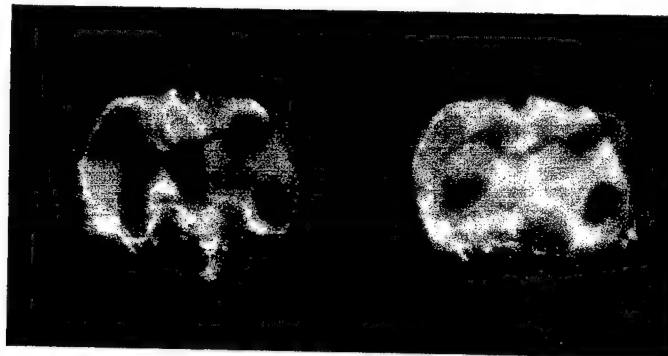
^{11}C-Glutamate

Figure 4. Volume rendered MR images fused with PET images showing temporal distribution of metabotropic glutamate receptor binding at 4 coronal brain levels in control rat brain. Scale t0 to t15 is continuous time scale. Acquisition time of each image was 15 s.

11C-Glutamate
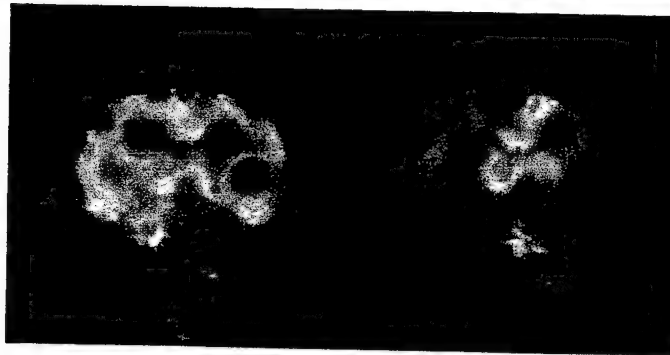
Figure 5. Metabotropic glutamate receptor binding pre and 3 days post 3-NP. Post 3-NP distribution was controlled with a study of glucose utilization. Metabotropic glutamate receptor binding is significantly deceased in striatum and some cortical areas.

PI. Anna-Liisa Brownell: "Evaluation of Early and Prolonged Effects of Acute Neurotoxicity Using Novel Functional Imaging Techniques"

Quinolinic Acid Lesioned Rat

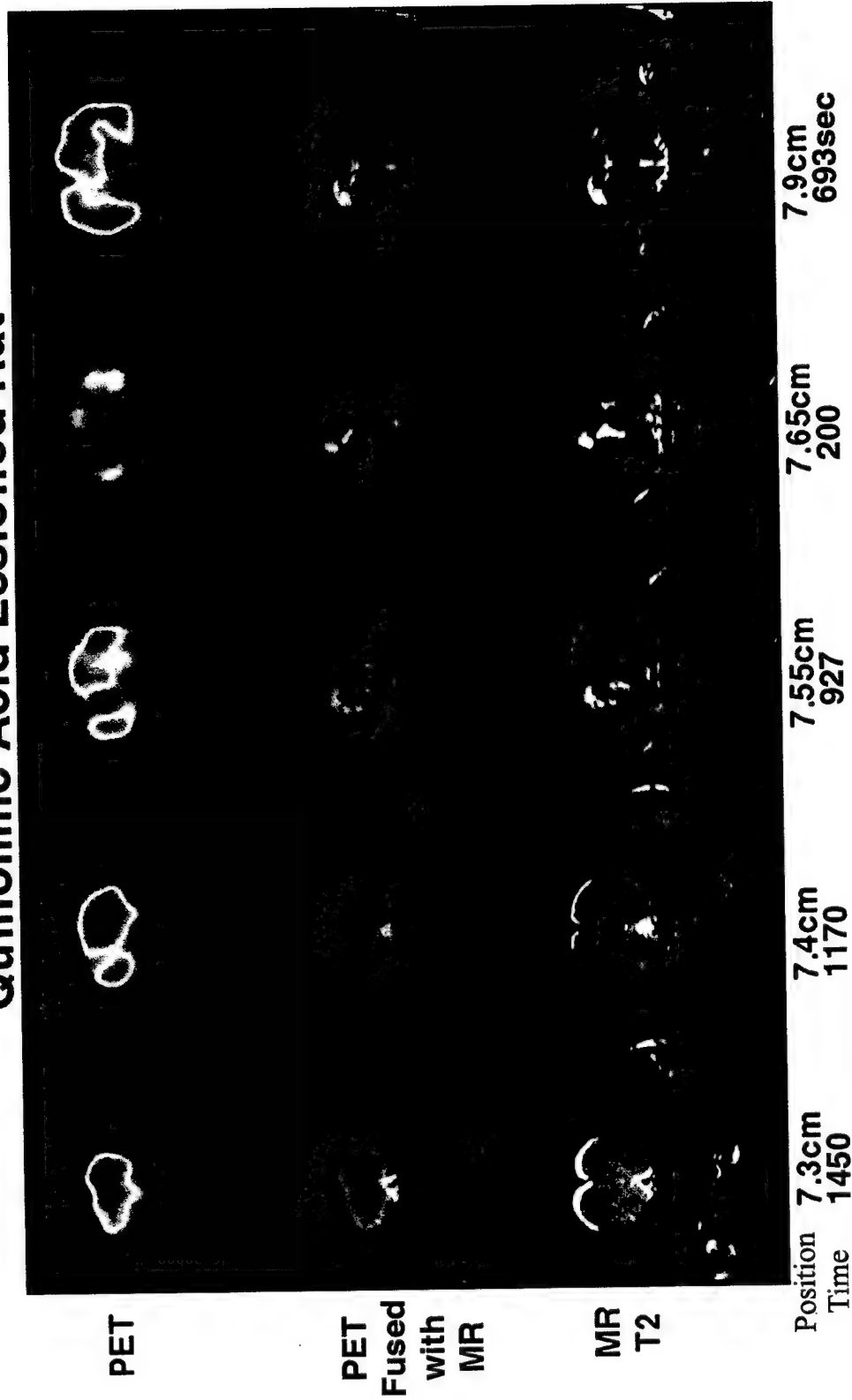| Position	7.3cm	7.4cm	7.55cm	7.65cm	7.9cm
Time	1450	1170	927	200	693sec

PET

PET Fused with MR

MR T2

Figure 6. PET imaging studies of glucose metabolism were conducted using ^{18}F-2-fluorodeoxy-D-glucose as tracer in a quinolinic acide lesioned rat. The glutamate binding was abolished at the lesioned striatum and cortex, compared to MR T2 weighted images.
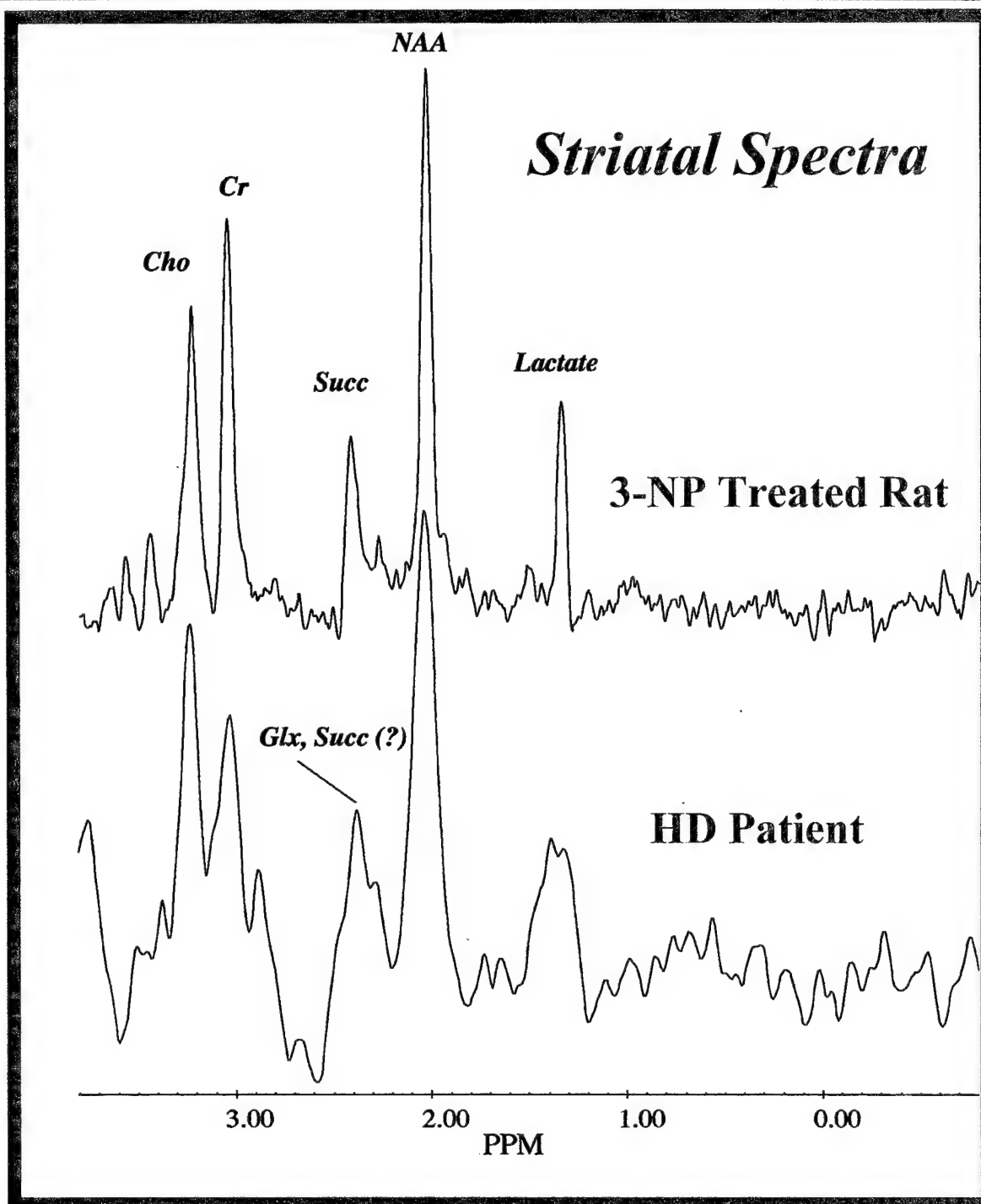
Figure 7. MR spectra of a rat striatum 2 days after 3-NP neurotoxicity with comparison to human Huntington's disease patient's striatum. Note the similarities of the two spectra and elevated peaks of succinate and lactate.
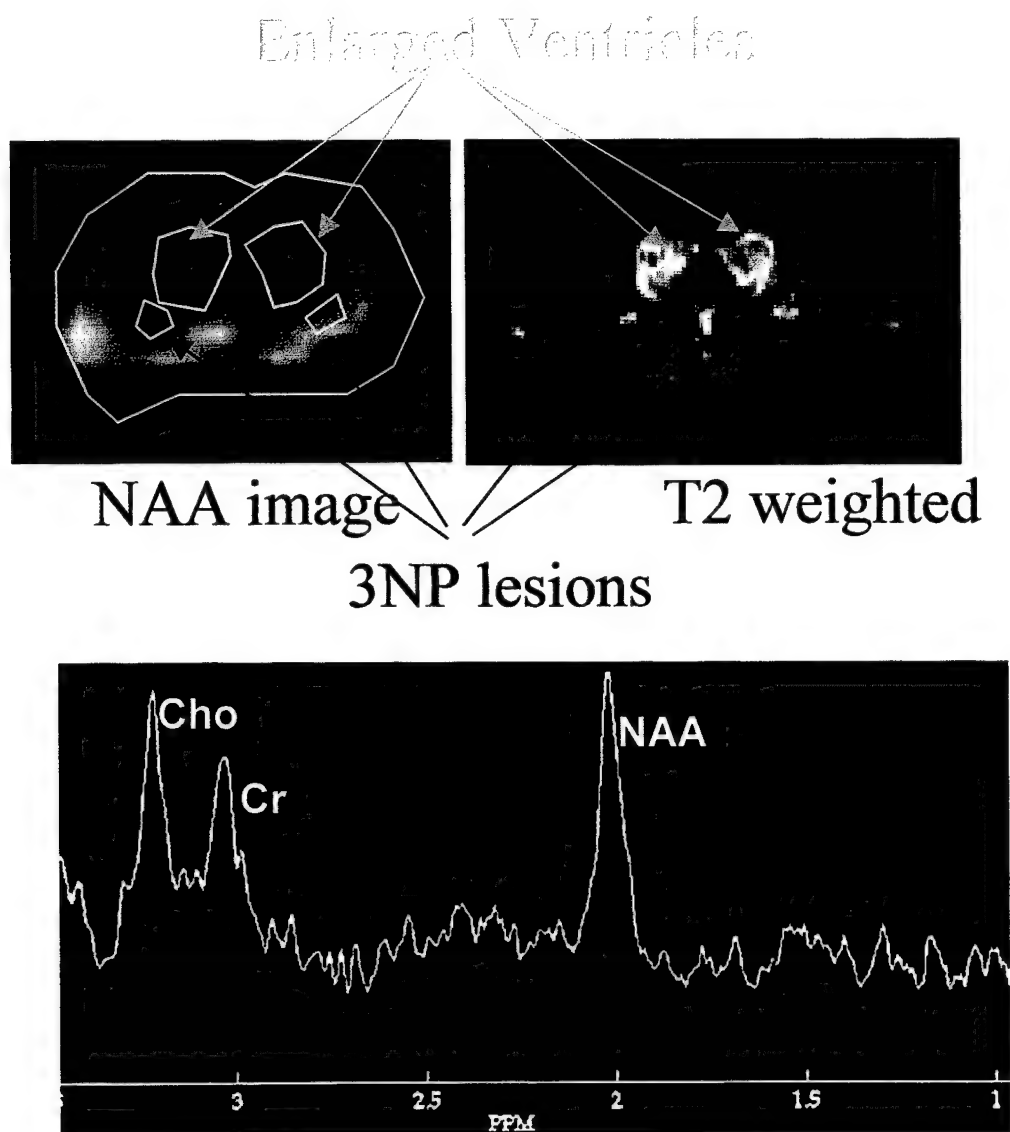
Figure 8. MRI T2 weighted image of the 3-NP treated rat shows enlarged ventricles and striatal lesions (bright spots). 2D MRS images shows decrease in NAA level in both ventricles and striata. 1D MRS over striata shows decrease in NAA level.

Figure 9. An endpoint study (2 days post 3NP treatment) of glucose utilization and its corresponding Nissl stained tissue cut present loss of the striatal function.
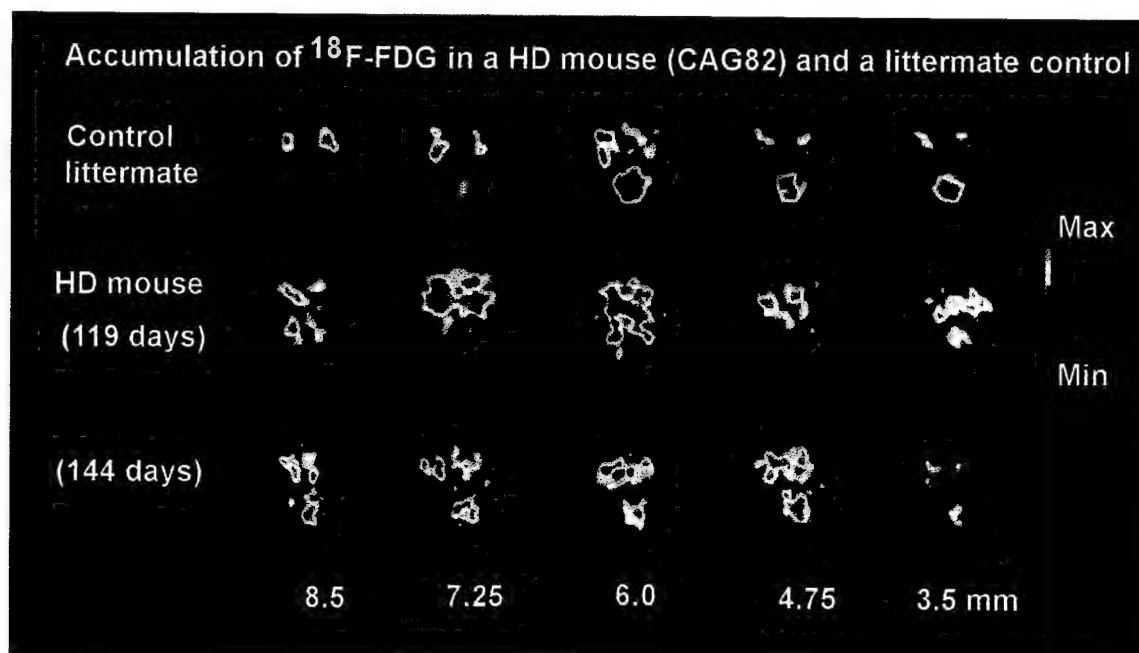
NAA Changes Over Time in Striatum in N82 and Wild Type HD Mice
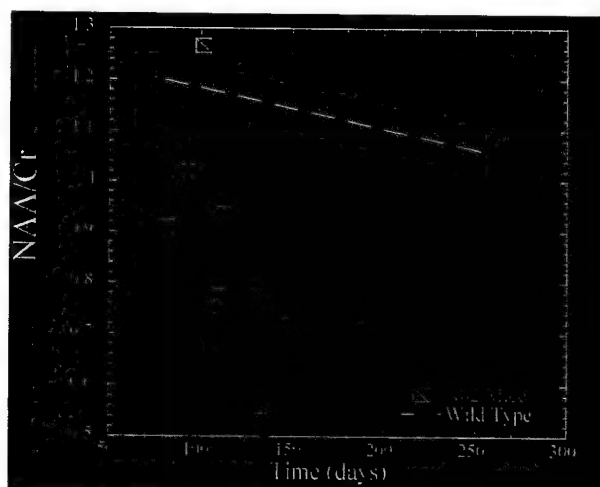
Figure 10. PET imaging studies of glucose utilization at 4 coronal brain levels in a control littermate and transgenic mouse (HD model, N82 mouse). Study of glucose utilization was repeated at two age points in HD mouse(above). MRS studies of NAA changes over time in N82 and wild type HD mice (below).

PI. Anna-Liisa Brownell: "Evaluation of Early and Prolonged Effects of Acute
Neurotoxicity Using Novel Functional Imaging Techniques"

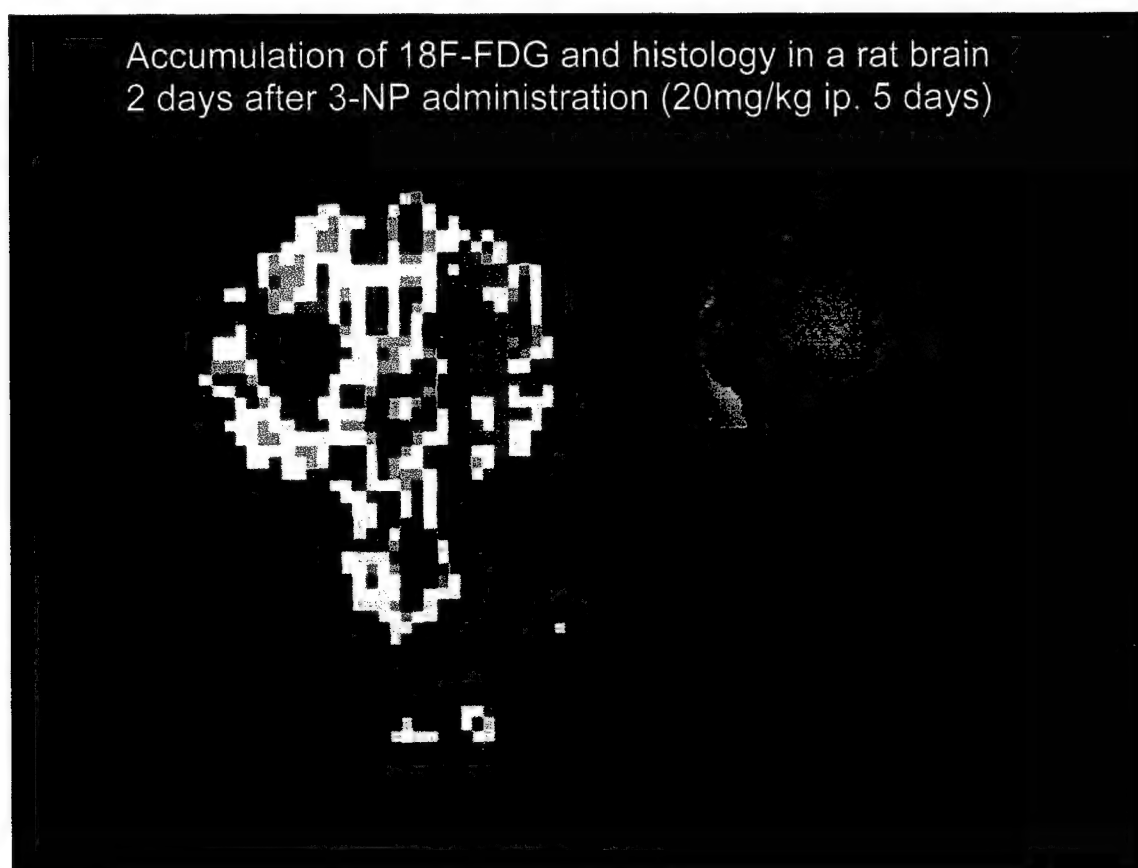## Typical MRS Voxels for Cortex and Striatum in Transgenic Mice

Average Voxel Size - 60 μL in striatum
-40 μL in cortex
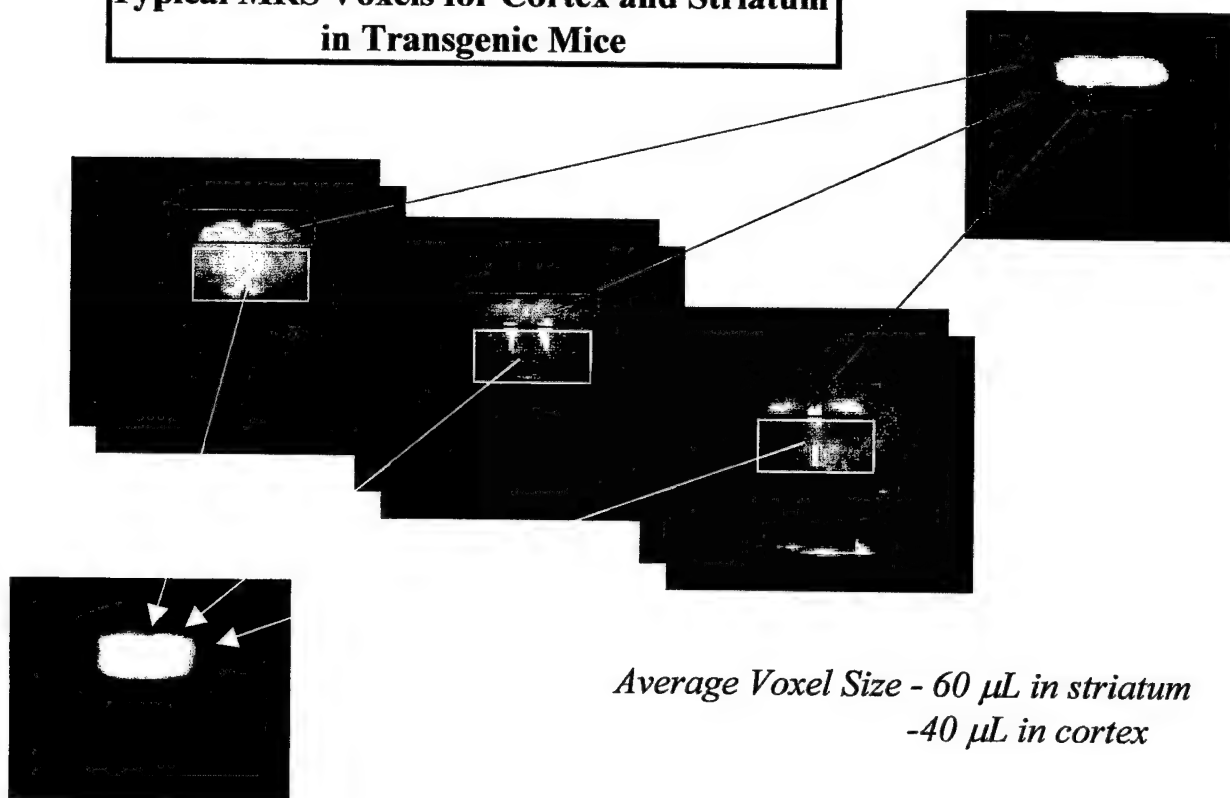
Selective NAA loss in Striatum in N82 HD Mice
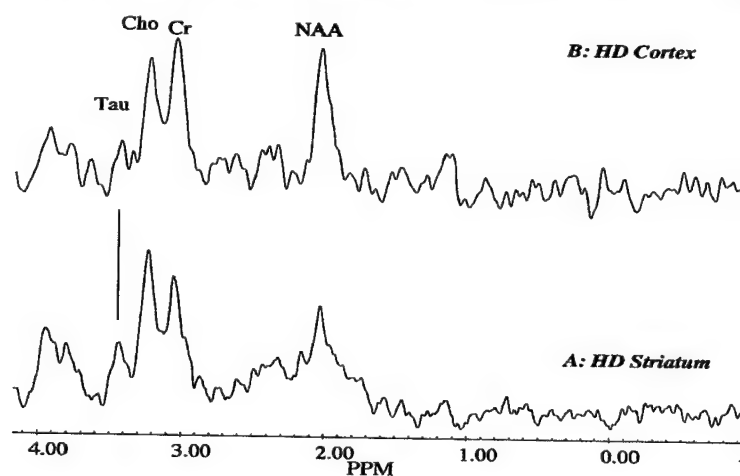
Figure 11. Selection of voxel for MR imaging in transgenic mouse (above). Integrated
signals inside selected voxels showing MR spectra for cortex and striatum in transgenic
HD (N82) mouse .

The Journal of Nuclear Medicine

JNM

THE 48TH SNM
ANNUAL MEETING

ABSTRACT BOOK

Scientific Abstracts of
the 48th Annual Meeting of
the Society of Nuclear Medicine
Toronto, Ontario, Canada • June 23-27, 2001

COUPLING OF GLUCOSE UTILIZATION TO NEURO-NAL TOXICITY—AN ULTRA HIGH RESOLUTION PET STUDY.

A.-L. Brownell, Y. I. Chen*, K. E. Canales, R. T. Powers, A. Dedeoglu, B. G. Jenkins, Dept. of Radiology, Massachusetts General Hospital, Boston, MA; Dept. of Mechanical Engineering, Massachusetts Institute of Technology, Cambridge, MA; Dept. of Neurology, Massachusetts General Hospital, Boston, MA. (200322)

**Objectives:** Increasing environmental toxicity has been significantly linked to the etiology of neurodegenerative diseases. To explore acute and long-term excitotoxically mediated mechanisms we used 3-nitropropionic acid (3-NP) in a rat model. Studies of cerebral glucose utilization (CGU) were conducted to explore 3-NP induced acute and chronic impact on energy metabolism. **Methods:** PET studies were carried out on an ultra-high resolution PET scanner (spatial resolution of 1.3mm, volume resolution of $2.1mm^3$). A total of 8 rats were injected with 3-NP (20mg/kg/day, i.p.) for 4 days. Behavior and body weight were monitored throughout the whole study. PET imaging of glucose metabolism was conducted daily during the 3-NP treatment period and 4 and 9 weeks after cessation of 3-NP injections. MR scans and histology were used to confirm the striatal lesioning. **Results:** A significant inter-animal variability in response to the 3-NP toxin was observed in neuroimaging studies and locomotor activity during the injection period. In the acute phase, 2 rats with hind limb paralyses showed a decrease in striatal CGU (40 ~ 50%). These rats, however, showed enhanced CGU in cortex (20~25%). Three rats with light motor symptoms developed smaller striatal lesions and had only a 10~15% decrease in CGU. The 3 rats with no motor symptoms did not develop striatal lesions and had no changes in CGU. The follow up studies at 4 and 9 weeks showed some recovery in CGU in the lesioned areas. Diffusion weighted MR scans and histological evaluation confirmed the lesions in those rats with motor symptoms. **Conclusion:** By using the ultra high resolution PET camera, it is possible to investigate 3-NP induced changes in cerebral glucose metabolism in a rat brain. We observed a compensatory mechanism of glucose utilization: the rats with highest decrease in striatal glucose utilization showed enhanced cortical levels. These studies may provide an understanding of the coupling of excitotoxicity to acute and long term biological and physiological changes and provide a means to develop possible neuroprotection.

3-NP induced neurotoxicity - assessed by ultra high resolution PET with comparison to MRI and MRS

A-L Brownell, YI Chen, KE Canales, RT Powers, A Dedeoglu, FM Beal, BG Jenkins

3-NP, a succinate dehydrogenase inhibitor, is widely used as an experimental model to study HD, energy metabolism and cell death. We used a rat model to investigate 3-NP induced acute and prolonged neurotoxicity using in vivo imaging of cerebral glucose utilization (CGU)and dopamine receptors by PET, neuroanatomy by MRI and neurochemicals by MRS. 3-NP was administered (male Spraque-Dawley) twice a day (10 mg/kg ip.) until symptomatic or max of 5 days. PET studies of CGU were conducted daily using a super high resolution (1.3x1.5x1.5 mm3) in-house built PET device. MRI and MRS studies were conducted with a GE Omega 4.7 T imager.

Studies of CGU showed significant inter animal variation in the acute response of toxin, similar to motor activity. The average decrease of CGU in the lesions was 31+/-12% and the lesions started to develop on the first day of 3-NP. Four weeks later CGU was recovered to -13+/-5% and then in 3 months decreased again to –48+/-10%. Dopamine D1 and D2 receptors showed progressively decreasing binding by PET after 3-NP using 11C-SCH and 11C-raclopride, respectively. However, the binding of dopamine transporter imaged by 11C-CFT showed early increase (1 week after 3-NP) followed by progressive decrease. MRS showed elevated peaks of lactate and macromolecules as well as succinate immediately after 3-NP toxicity which diminished in 4 months, indicating a reversible process. Choline peak increased and N-acetylaspartate peak decreased in 4 months indicating loss and damage of neurons. Post mortem histological studies confirmed the neural loss.

HiRes 2001

High Resolution Imaging in Small Animals:
Instrumentation, Applications and Animal Handling

**Doubletree Hotel and Executive Meeting Center
Rockville, Maryland, USA
September 9-11, 2001**

Sponsored by:

**The National Cancer Institute
The Society for Molecular Imaging
Oak Ridge Associated Universities
The Academy of Molecular Imaging
Society for Non-Invasive Imaging in Drug Development
Bruker Medical Incorporated
CTI / PETNET
ImTek Incorporated**

Web site served by Oak Ridge National Laboratory | Disclaimer |

GLUCOSE UTILIZATION ASSESSED BY HIGH RESOLUTION PET WITH COMPARISON TO MRI/MRS IN A TRANSGENIC MOUSE MODEL OF HUNTINGTON'S DISEASE

Anna-Liisa Brownell[1], Y. Iris Chen[2], Kelly Canales[1], Robert Powers[1], Ole Andreasson[3], Flint Beal[3], Bruce Jenkins[2]

[1]Massachusetts General Hospital, Department of Radiology, Bartlett Hall 500R, Boston, MA 02114, [2]Massachusetts General Hospital, NMR Center, Charlestown, MA 02129, [3]Massachusetts General Hospital, Department of Neurology, Boston, MA 02114.

Summary: We conducted longitudinal studies of glucose utilization and neurochemicals in a transgenic mouse model of Huntington's disease (HD) and littermate controls using high resolution PET and MRI/MRS techniques. Glucose is a sensitive marker of tissue energy metabolism, N-acetylaspartate (NAA) is a marker of neuronal health and choline (Cho) may be an indicator of gliosis. In the striatum of HD mice, a progressive linear decrease of glucose utilization and an exponential decrease in NAA was observed. The percent decrease in striatal NAA (compared to the wild-type animals) was two times higher than the percent decrease in glucose utilization. These observations parallel with the development of HD symptoms. In conclusion, this transgenic mouse model provides an excellent model for efficient study of human disease and high resolution in vivo imaging techniques provide unique quantitative approach to investigate pathophysiological processes in small animal models.

Introduction: After discovery of gene related diseases and development of different animal models to mimic the human diseases, a lot of pressure has come to develop in vivo imaging techniques, first to develop diagnostic methods to investigate pathophysiological processes and second to develop therapies for them. Recent advances in molecular engineering provide a direct animal link between human disease and transgenic mouse models to study pathophysiologic parallels and human-like response in transgenic mice. We investigated a transgenic mouse model of Huntington's disease. HD is an autosomal dominant inherited neuropsychiatric disease that usually starts at middle age and inevitably leads to death. The disease mutation consists of an unstable expanded glutamine trinucleotide repeat, coding region of the gene that encodes a stretch of polyglutamines. In humans, repeat length of >70 produce juvenile onset of HD. We used a transgenic mouse model of 82 CAG repeat. These mice develop normally, but about 6 weeks of age they show loss of brain and body weight, and around 9-11 weeks, develop many of the features of juvenile HD.

With newly developed high resolution in vivo imaging techniques it is possible to obtain information of the progression of the degeneration in different brain areas. This information is essential in evaluating overall pathophysiological processes as well as in developing therapies.

We have at the Massachusetts General Hospital, a long standing strong instrumentation development program accompanied with special software development program for special needs. These tools have been fundamental to develop applications in small animal models. PET studies in this application were done with an ultra high

resolution in house built single ring PET scanner (resolution 1.3 x 1.3 x 1.8mm, 3.0 μl) connected to computer controlled imaging table. MRI/MRS studies were done with GE Omega 4.7 T imager.

Methods: We did PET imaging studies of glucose utilization and MRS studies of neurochemicals including N-acetylaspartate and choline in 30 transgenic mice with 82 CAG repeat and in 8 littermate controls. Imaging studies were conducted when the mice were 80-130 days old. For imaging studies mice were anesthetized using halothane (1.5-2.5% with oxygen flow rate of 1.5 L/min) and adjusted into a house built stereotactic head frame. For PET studies tail vein and artery were catheterized for administration of radioactivity and getting blood samples. Catheters were prepared of pediatric polyethylene tubing PE 10 (diameter of .011") and a needle size of 30G. Glucose concentration was determined of arterial blood and/or mixed venous and arterial blood of cut tail tip. After injection of ^{18}F-fluorodeoxy-D-glucose (2FDG) (2-3 mCi) dynamic data were acquired for 20 min at the midlevel of heart and brain sequentially moving the imaging table back and forth between the two sites to obtain data of washout of radioactivity from blood and accumulation into the brain. The blood input function can be detected of the tiny region of interest located inside the left ventricle. However, this data include spillover of the radioactivity accumulated in the heart muscle. To correct for this spillover 4 blood samples were taken from the cut tail tip between 1 and 20 min. When the steady state of radioactivity was reached, sequential scanning over the brain was done using 1.25 mm steps. Data were corrected for uniformity, sensitivty, and attenuation and images were reconstructed using Hanning filtered convolution backprojection with cut off value of 1.0. PET data were corrected for acquisition time, decay and injected dose and images were fused with MR images and volumetric region of interest including striatum and motor cortex were drawn based on MRI and anatomical atlas. Average radioactivity per voxel was calculated in striatum and motor cortex. Glucose metabolic rate was calculated using the Sokoloff model and a value 0.5 for the lumped constant.

In vivo MRS was acquired using a PRESS sequence and TR of 2000ms and three TE values (68,136, and 272 ms). Voxels were placed symmetrically over both basal ganglia (average size of 6x3.5x3 mm, 63μl) or over the motor cortex (6x2x3mm, 36μl). Spectra were analyzed using the NMR1 software program (New Methods Research, Syracuse, NY). Spectra were integrated and normalized to the creatine/phosphocreatine peak.

Results:

18F-2FDG study in a control mouse

10.0   8.75   7.5   6.25   5.0   3.75   2.5   1.25 mm
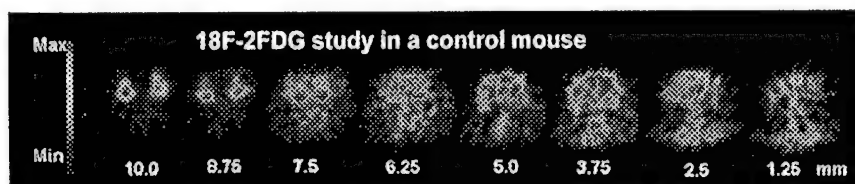
Above is an image of 2FDG distribution in 8 coronal brain levels in a littermate control mouse. Longitudinal analyses of glucose utilization in HD mice showed in striatum a progressive decrease of 0.05%/day. The decrease in striatal NAA was one order higher being 0.56%/day. In the same time period Cho was increased 34 % compared to

3

littermate control. These observations parallel the developing of HD symptoms. Interestingly, no significant changes were found in cortical metabolism.

Discussion: In vivo high resolution quantitative imaging techniques can provide longitudinal information of multiple simultaneous processes in natural biological environment. This is the most important factor compared to in vitro techniques, which can provide brief information of isolated biological problems ignoring biological interaction created by the surrounding tissues and elements. These preliminary studies of glucose utilization and neurochemicals in a transgenic mouse model of Huntington's disease clearly demonstrate that this transgenic mouse model provides an excellent model for efficient study of human disease.

Multiresolution Estimation

T. Cao-Huu and A-L. Brownell

Abstract— We are interested in automatic estimation algorithms that provide not only estimates of the boundaries and of the regions of interests, but also statistics for the errors in the estimates.

In this work, estimation is thought of as a variational formulation of the segmentation problem. We minimize a functional, which is posed for segmentation, over a class of admissible functions while incorporating efficient Bayesian estimators by a prior model. Our multiresolution, Krylov subspace framework is computationally efficient and can result in optimal estimates of important neurophysiological processes.

Keywords— Multiresolution, Krylov subspace, segmentation, statistical estimation, calculus of variation.

I. MOTIVATION

This work arose from the need to develop an automatic algorithm to provide not only estimates of the boundaries and of the regions of interests (ROI), but also statistics for the errors in the estimates. Of particular interest to us are regions-of-interest imaging methods with varying resolution to obtain, for example, accurate inputs of quantitative models of physiologically important processes such as the density and kinetics of neuroreceptors[1]. In practice, we have used anatomical data (MRI/CT) to define ROIs from true volumetric PET data, rather from slices of the brain. Quantitative measurements of the quality of the estimates are important in order to reduce bias and error propagation, especially with the ever increasing volumes of 3D/4D data sets from the state-of-the-art, and multi-modal imagers.

We think of estimation (reconstruction) as a variational formulation of segmentation. That is, we wish to minimize a functional, which is posed for segmentation, over a class of admissible functions while incorporating Bayesian estimators with a prior model that are capable of generating error statistics and yet is computationally efficient. Estimating the magnitudes of the errors is natural in the Bayesian statistical framework.

We are particularly interested in methods based on models with relatively simple statistical interpretations. Developing statistical interpretations of variational problems is not new. However, most current Bayesian estimators employ the Markov random field priors which are well known to require an unacceptably large number of computations in order to produce good estimates, especially for two-dimensional and three-dimensional processes evolving in time. We adopt instead multiresolution prior models in our strategy and cast the reconstruction problem in a statistical framework for segmentation. To further reduce computation, we have developed estimation algorithms based on Krylov-subspace pixel basis decomposition to provide stability for infinitely-dimensional discrete-time Kalman filters whose states are elements in Hilbert space.

II. BACKGROUND AND SIGNIFICANCE

Calculus of variation is a collection of mathematical tools for optimization over a function space. Its centerpiece is a cost functional, a scalar mapping from a set of candidate functions. The functional captures the essence of a problem and, essentially, orders the candidates by the criteria implied by the form of the functional [2]. Mumford and Shah [3], [4] have proposed formulating the image segmentation problem as the minimization of the following functional:

$$E(c,B) = \int \int_{\Omega} r^{-1}(g-c)^2 dx dy + \\ \lambda \int \int_{\Omega-B} |\nabla c|^2 dx dy + \beta |B| \tag{1}$$

where $\Omega \subset \mathbf{R}^2$ is the image domain, $g : \Omega \to \mathbf{R}$ is the image data, $c : \Omega \to \mathbf{R}$ is a piecewise

[1]The neuro-imaging laboratories at the Massachusetts General Hospital, under the auspices of Prof. A-L. Brownell, study the effects of toxicity and/or neuroprotection on oxidative glucose metabolism in the brain and on binding of specific neuroreceptors.

smooth approximation to g, $B \subset \Omega$ is the union of segment boundaries, and $|B|$ is the length of B. The first term places a penalty on deviations of c from the data g; the second term ensures that c is smooth except at edge locations; and the third term penalizes spurious edges. The constants r, λ and β control the degree of interaction between the terms. Mumford and Shah's functional (1) has many beautiful mathematical and psychovisual properties [2], but its use for segmentation has been severely limited because the difficulty in computing minimizers due to the discrete nature of the edge term, $\beta|B|$. Since a related functional can be used to process noisy images, we can obtain a smooth approximation of the original image by finding the minimizer of

$$
\begin{aligned}
E(c) &= \int (r^{-1}(g-c)^2 + \lambda|\nabla c|^2)dxdy \\
&= r^{-1}||g-c||^2 + \lambda||\nabla c||^2
\end{aligned}
\tag{2}
$$

where g is the raw image intensity data, r and λ are positive constants, and $||\cdot||$ denotes the standard L^2-norm of functions, then the candidate function that minimizes (2) is a smoothed version of the raw image. The first term of this functional penalizes deviations from the original image, and the second term ensures that the minimum of (2) is smooth. The degree of smoothing depends on the relative weighting of the data and gradient terms. The larger λ/r^{-1} is, the smoother the result.

In the context of image reconstruction using a generalized natural pixel basis[2], a least squares estimator (LSE) can be formulated to estimate the mean intensity of the generalized pixels, $\hat{c}$, used to described the unknown spatial distribution from one measured projection dataset, $\boldsymbol{p}$. The least squares estimator for the mean intensity of the generalized pixel image is found by minimizing the square of the L_2 norm of the difference between the projection vector, $\boldsymbol{p}$, and the estimated projection, $F \cdot B^T \boldsymbol{c}$, over all possible image vectors, $\boldsymbol{c}$,

$$
\hat{\boldsymbol{c}} \equiv \arg\min_{\boldsymbol{c}}\left\{ \left\| \boldsymbol{p} - F \cdot B^T\boldsymbol{c} \right\|_2^2 \right\}.
\tag{3}
$$

Finding the gradient vector with respect to unknown parameters, $\boldsymbol{c}$, and equating it with the

[2]Pleasee see for example Hsieh *it al* [1].

zero vector, yields a $\Theta K \times \Theta K$ system of simultaneous linear equations whose solution is

$$
\hat{\boldsymbol{c}} = \left(S \cdot V^T \cdot B^T\right)^+ \boldsymbol{U}^T\boldsymbol{p}.
\tag{4}
$$

In the variational context, we consider the discrete form of (2),

$$
E(c) = r^{-1}||g-c||^2 + \lambda||Lc||^2,
\tag{5}
$$

where c and g are elements in a finite dimensional real vector space, $||\cdot||$ represents the Euclidean norm, and L is a linear operator. The least squares estimator for the mean of the intensity in continuous space is found by applying the adjoint of the basis operator, B, to the generalized pixel estimator of the intensity mean.

$$
\hat{b} = B^T\hat{\boldsymbol{c}} = B^T\left(S \cdot V^T \cdot B^T\right)^+ \boldsymbol{U}^T\boldsymbol{p}.
\tag{6}
$$

And their the estimators and covariance are,

$$
\hat{\boldsymbol{c}} = \left[\left(S \cdot S^T\right)^+\right]^{\frac{1}{2}} \boldsymbol{U}^T\underline{\boldsymbol{p}}
\tag{7}
$$

$$
\boldsymbol{\Sigma}_{\hat{\boldsymbol{c}}} = \left[\left(S \cdot S^T\right)^+\right]^{\frac{1}{2}} \boldsymbol{U}^T\boldsymbol{\Sigma_p}\boldsymbol{U}\left[\left(S \cdot S^T\right)^+\right]^{\frac{1}{2}}
\tag{8}
$$

$$
\hat{b} = V \cdot S^T\left(S \cdot S^T\right)^+ \boldsymbol{U}^T\underline{\boldsymbol{p}}.
\tag{9}
$$

The function $\hat{c}$ that minimizes (5) is also the solution to finding the Bayes least-squares estimate of a process c whose measurement equation is

$$
g = c + \sqrt{r}v
\tag{10}
$$

and whose prior probabilistic model is given by

$$
\sqrt{\lambda}Lc = w,
\tag{11}
$$

where v and w are independent white Gaussian random vectors with identity covariance.

The result is a robust method to remove noise from an image, effectively having a regularizing effect on ill-posed inverse problems by filtering out eigencomponents of the solution belonging to the noise subspace. But the drawback is that edges are blurred. We avoided this by introducing edge terms which prevent smoothing near the edge. Such functionals can be used to produce a segmentation.

A. Krylov-subspace singular values filtering

Small singular values in (7) lead to large statistical errors in the reconstructed image, $\hat{b}$. A weighting matrix, D, can minimize the mean square error of the estimates. We determine its weighting values in the Krylov-subspace.

$$D_{j'j} = \begin{cases} 1 & \text{if } j' = j \text{ and } j < J, \\ 0 & \text{otherwise} \end{cases} \quad (12)$$

will select only the J largest singular values. Thus our algorithms have a regularizing effect on ill-posed inverse problems by filtering out eigencomponents of the solution belonging to the *noise subspace*. An approximation b^δ to b is

$$b^\delta = \sum_{k,\,\sigma_k \geq \sigma} \frac{1}{\sigma_k}(p^\delta, p_k)b_k, \quad (13)$$

where $\sigma = \sigma(\delta)$ plays the role of a regularization parameter in the Krylov subspace of dimension k.

We let g_{ij}, c_{ij}, and s_{ij} be samples of g, f, and s respectively on an $n \times n$ rectangular grid, and to approximate the gradient by a first difference scheme and then use coordinate descent for minimization so that each of the subproblems will have a simple structure. In n-dimensions, the samples are arranged in a lexicographic ordering into column vectors g, c, and s. We define a $2n(n-1) \times n^2$ matrix $\mathcal{L}$ to act in analogy to the gradient operator. The first differences along rows of image pixels are taken by multiplication by the $(n-1) \times n$ matrix L_r. To compute the first differences of all rows of an image, we use the operator $\mathcal{L}_r$, composed of n blocks of L_r, along its diagonal. Then we compute the first differences of all columns of the image by operating with $\mathcal{L}_c$. Finding the minimizer $\hat{c}$ and their error variances involves solving

$$(r^{-1}I + \mathcal{L}^T \mathcal{S}^T \mathcal{S} \mathcal{L})\hat{f} = g \quad (14)$$

and finding the diagonal elements of $((A^T A)^{-1} + \mathcal{L}^T \mathcal{S}^T \mathcal{S} \mathcal{L})^{-1}$. Finding the minimizer $\hat{s}$ and its error variances can be done similarly.

There exist *no known* algorithms which can compute the necessary quantities for this general problem with fewer than $O(n^3)$ multiplications. Iterative methods can compute $\hat{x}$ with fewer than $O(n^3)$ multiplications, but computing the diagonal elements of the inverse requires at least $O(n^3)$

multiplications by known algorithms. We perform Kalman filter smoothing to calculate optimal estimates and error variances for an $n \times n$ image with $O(n^2)$ multiplies in Krylov subspace.

B. Multiresolution and Overlapping Domains

We adopt techniques known in the scientific computing and numerical analysis as 'overlapping domain decomposition' to design an algorithm that is fast and can possibly achieve constant computational complexity per pixel. These techniques can deliver optimal performance by creating locality of reference (through algebraic restructuring) and exploiting the architecture of the computing machines for infinite-dimensional discrete-time Kalman filters whose states are elements in Hilbert space. Figure 1(left) shows domain Ω_1, domain Ω_2 and their overlapping nodes; while Figure 1(right), the coarse and fine discretizations allowing finer resolution images at specific domains. This renders the computation feasible in practical situations. The overlap region $\Omega_1 \cap \Omega_2$ is a nonzero fraction of the total domain $\Omega_1 \cup \Omega_2$, as long as the number of iterations required for convergence is independent of h as h goes to zero. In practice we would want to use many domains, especially on parallel processors. Suppose we have
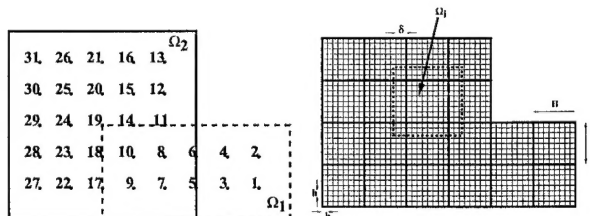

Fig. 1. (Left) Domain Ω_1, domain Ω_2 and their overlapping nodes; (Right) Coarse and fine discretizations allowing computation of finer resolution over a portion of an image.

many domains Ω_i, each of size $H \gg h$. If we let $\delta < H$ be the amount by which adjacent domains overlap, and H, δ and h all go to zero, such that the overlap fraction δ/H remains constant, and $H \gg h$, then the number of iterations required for convergence grows like $1/H$. So we can use an approximation A_H of the problem on the coarse grid with spacing H to get a *coarse grid preconditioner* in addition to the fine grid preconditioners $A_{\Omega_i,\Omega_i}^{-1}$. We need three matrices to describe the algorithm. First, let A_H be the matrix for the model problem discretized with coarse mesh spacing H.

Second, we need a *restriction operator R* to take residual on the fine mesh and restrict it to values on the coarse mesh. Finally, we need an *interpolation operator* to take values on the coarse mesh and interpolate them to the fine mesh, R^T.

We model an image as the finest scale of a stochastic process indexed by nodes on a quad tree. The statistics of this process are defined in terms of a recursion on the tree. An abstract index ν is used to specify a particular node on the tree, and the notation $\nu\bar{\gamma}$ is used to refer to the parent of node ν. A process that lives on the tree has a state variable x_ν at every node and is defined by a root-to-leaf recursion of the form

$$x_\nu = A_\nu x_{\nu\bar{\gamma}} + B_\nu w_\nu \qquad (15)$$

where the w_ν and the state x_0 at the root node are a collection of independent zero-mean Gaussian random variables, the w's with identity covariance and x_0 with some prior covariance P_0. The A and B matrices are deterministic quantities which define the statistics of the process on the tree. Observations g_ν of the state variables have the form

$$g_\nu = C_\nu x_\nu + v_\nu \qquad (16)$$

where the v_ν are an independent collection of Gaussian random variables, and the matrices C_ν are deterministic quantities which specify what is being observed. The Bayes least-squares estimates of process values at all nodes on the tree given all observations and the associated error variances can be calculated with a faster and efficient recursive algorithm which requires only $O(n^2)$ multiplications when there are $n \times n$ finest scale nodes.

III. Some results and discussion

The multiresolution framework allows efficient computation of finer resolution over specific portions of an object rendering the computation feasible for high resolution ROI imaging. The strategy described above is used to arrive at approximate solutions to the problems of estimating c and s in the coordinate descent segmentation scheme. Each of the coordinate descent sub-problems is a convex quadratic minimization problem amenable to a precise statistical interpretation. Our algorithms compute both these estimates and their associated error variances, which are shown in Figure 2. Note that the edge estimate $\hat{s}$ highlights so

clearly the boundary between the gray and white matter. Monte Carlo experiments have also indicated that the estimates and error statistics are accurate and provide meaningful quantities.

There are many possible extensions of this work on several different fronts. One is on variational formulation of how to extract boundaries from a continuously varying edge estimate. Another is on statistical interpretation of how to precisely relate, via simulation or analysis, the calculated error statistics with actual error statistics of interest. Experimentation with PET, MRI and CT data are currently under way to understand how to better formulate models that precisely incorporate inhomogeneities.
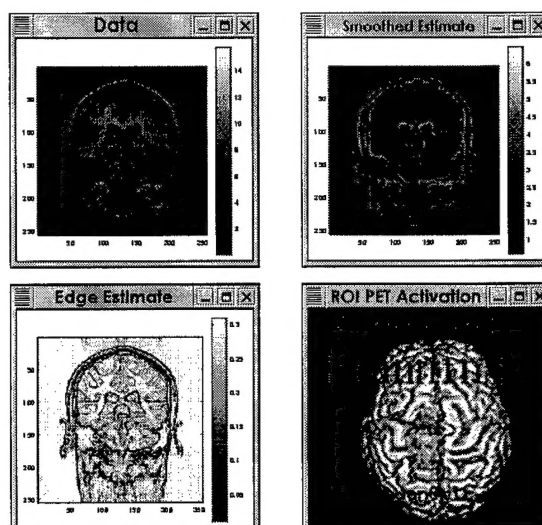

Fig. 2. (Top left), Data. (Top right), Smoothed estimate error standard deviations. (Bottom left), Edge estimate error standard deviations. (Bottom right), Brain activation using MRI data to define ROI's from PET volumetric data. Yellow defines tumor volume.

References

[1] Y. L. Hsieh, G. T. Gullberg, G.L. Zeng, and R.H. Huesman. An svd reconstruction algorithm using a natural pixel representation of the attenuated radon transform. *IEEE Trans Nucl Sci*, 43(1):2306–2319, 1996.

[2] J. Morel and S. Solimini. *Variational Methods in Image Segmentation*. Birkhäuser, Boston, 1995.

[3] D. Mumford and J. Shah. Boundary detection by minimizing functionals, I. In *Proc. IEEE Conference on Computer Vision and Pattern Recognition*, pages 22–26. IEEE, 1985.

[4] D. Mumford and J. Shah. Optimal approximations by piecewise smooth functions and associated variational problems. *Communications on Pure and Applied Mathematics*, 42:577–684, 1989.